SOLAR SYSTEM

80 MHz Observations of the Coronal Broadening of the Crab Nebula

J. R. HARRIES, R. G. BLESING AND P. A. DENNISON
Department of Physics, University of Adelaide

Regions of the interplanetary medium currently inaccessible to space vehicles may conveniently be studied using the radio scattering properties of the interplanetary plasma. These effects may give rise to angular broadening[1, 2, 3] of radio sources sufficiently close to the Sun, or to amplitude scintillation [4, 5] of sources of small angular size.

In this note we report observations of the coronal broadening of the Crab nebula during June 1969 using the CSIRO radioheliograph at Culgoora. Observations of the degree of broadening and the size and orientation of the broadened image of the source give information about the irregularities in electron density in the corona. Previous work,[1] carried out using interferometers, has indicated some anisotropy in the scattered distribution. The interpretation of this effect has, however, been limited by the nature of the observations, which were unable to yield a complete brightness distribution of the source. In this paper we present the first direct two-dimensional images of the broadened Crab nebula at 80 MHz.

The radioheliograph, in its normal mode of operation,[6] produces a picture of a 2° square area of sky, at 80 MHz, every second. The picture is made up of an array of picture 'points' separated by 2′.13 at the zenith. The beam has a half-power width of 3′.9 in the zenith with a grating response at about 2°. Data were recorded on film and also on digital magnetic tape. The picture repetition rate of $1s^{-1}$ is sufficient to enable effects of solar activity to be readily identified and will allow the investigation of short time variations in the scattering. Pen recordings were also taken by leaving the heliograph beams fixed and allowing the source to drift through the 48 independent declination beams. The signals from up to 9 of these beams were recorded depending on the degree of broadening of the source.

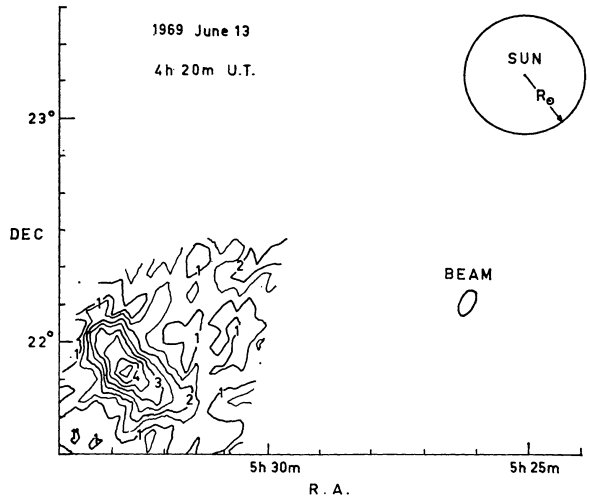

Figure 2. A contour diagram of the Crab nebula on June 13 showing the relationship of the source to the Sun.

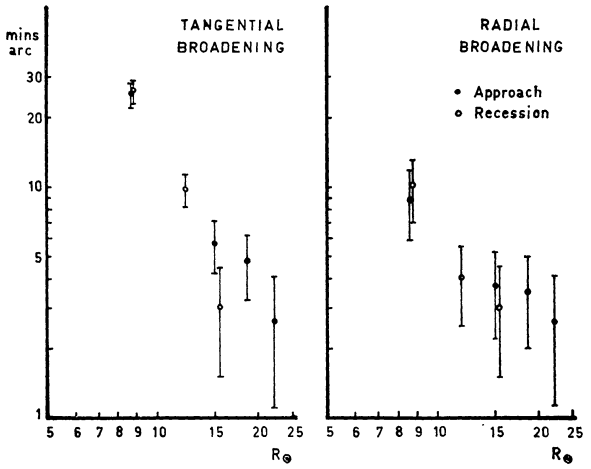

Figure 3. Scattering angle (full width at half maximum) in the radial and the tangential direction as a function of heliocentric distance.

Figure 1* shows a series of photographs taken throughout the observing session, each representing an integration of 8 one-second pictures. From May 30 to June 8 the image was consistent with the inherent source size and the beam shape. On June 9 some short-term broadening, possibly related to solar activity, was observed. The broadening became established on June 11 throughout most of the day's observations; on the 12th no observations were possible due to a noise storm on the Sun. On June 13 the source was seen to be considerably enlarged with a roughly elliptical distribution, and a contour diagram of the source on this day is shown in Figure 2. The broadening is anisotropic, being about 2.5 times greater in the tangential than in the radial direction from the Sun. On June 14, 15 and 16 the source could not be detected above the background on the film. For these days attempts are being made to resolve the source using the magnetic tape data by integrating over longer periods, but as yet no conclusive results have been obtained. The source was again visible on June 17 and seen to be broadened—again, predominantly in the tangential direction. Broadening was still present on the 18th and 19th but after this became more sporadic and eventually disappeared.

For multiple scattering of the radio waves the angular spectrum of the scattered distribution may be taken to have the form $\exp(-\theta^2/\theta_s^2)$, where θ_s is the rms scattering angle. θ_s is proportional to (ϕ_0/l), the ratio of the rms phase deviation and the size of the irregularities. A preliminary analysis has been carried out assuming the image to have an elliptical form with Gaussian cross-sections as above. The method of least squares was used to fit such a distribution to the observed image, calculating the position of the source, the scattering angle along the major and minor axes, and the orientation of the ellipse. In each case the ellipse was found to be oriented with its

*See Plate II.

major axis almost normal to the radial direction from the Sun. Figure 3 shows the scattering angle in both the radial and the tangential directions as a function of heliocentric distance. Results from both the magnetic tape data and pen recordings are combined in the figure.

The elongated image is related to the shape and size of the irregularities of electron density in the corona. The enhanced broadening in the tangential direction indicates an elongation of the scattering irregularities in the radial direction. Such elongation might occur as a result of plasma diffusion being inhibited across the radial magnetic field in the scattering region. Some of the pictures have shown the broadened image to be curved along an arc centred on the Sun, which tends to confirm the radial elongation of the plasma irregularities.

The results presented here are preliminary and work is continuing which we hope will help to elucidate the relation between the scattered distribution and the nature of the plasma irregularities. The analysis of short-period variations in the broadening and apparent flux of the source and their relation to solar activity, and also the effect of different polarizations, will be described elsewhere.

It is a pleasure to thank the CSIRO Division of Radiophysics and Dr J. P. Wild for their assistance and cooperation in our use of the radioheliograph. This work forms part of a research programme in radioastronomy at the University of Adelaide, supported by the Australian Research Grants Committee (Grant B68/17014). Two of us (R.G.B. and J.R.H.) acknowledge the support of a Commonwealth Postgraduate Award and a Queen Elizabeth II Fellowship respectively.

[1] Hewish, A. and Wyndham, J. D., *MNRAS*, **126**, 469 (1963).
[2] Slee, O. B., *Aust. J. Phys.*, **12**, 134 (1959).
[3] Erickson, W. C., *Ap. J.*, **139**, 1290 (1963).
[4] Dennison, P. A. and Hewish, A., *Nature*, **213**, 343 (1967).
[5] Dennison, P. A., *Planet Space Sci.*, **17**, 189 (1969).
[6] Wild, J. P. *et al.*, *ProcIREE Aust.*, **28**, No. 9 (1967).

On the Radio Frequency Spectrum of Jupiter

L. J. Gleeson, M. P. C. Legg and K. C. Westfold
Monash University, Melbourne

Recent observations[1, 2, 3] of the radio-frequency flux spectrum of Jupiter in the frequency range 80-10 000 MHz suggest that the synchrotron component is not independent of frequency as has been generally accepted. Rather, the flux decreases at frequencies below 300 MHz and above 3000 MHz. In this paper we show that extensions and variations of the well-known dipolar model for this emission can account for the modified spectrum.

Models which account for the observed intensity and polarization characteristics are based on the planet having a dipolar magnetic field in which electrons of rest mass E_0 are trapped.[4, 5, 6, 7] The electron guiding centres are assumed to lie on a surface generated by rotating a magnetic field around the dipole axis. The equatorial radius of this surface r_e is three Jovian radii; the equatorial magnetic induction is B_e and the corresponding cyclotron frequency f_e. A rocking of the plane of polarization is accounted for by assuming that the dipole axis and the rotation axis are displaced by some 10°.

The frequency spectrum of the total flux to which these models have hitherto been matched is that of Figure 1 in the review by Roberts.[4] It extends down to 200 MHz and, to obtain the synchrotron component, the observed flux has been corrected for black body radiation of 140°K from the disk of the planet. This frequency spectrum has been interpreted as having zero slope and accounted for by assuming the electrons to be distributed in total energy E according to $(E/E_0)^{-\gamma}$ with the energy spectral index $\gamma = 1$. This distribution, in general, leads to a frequency of dependence of $f^{-(\gamma-1)/2}$ providing $f_c(E_1) \ll f \ll f_c(E_2)$, where $f_c(E)$ is the critical frequency[8] at energy E, and E_1 and E_2 are the lower and upper limits on the energy distribution. Reasonable agreement with the observed linear polarization characteristics is obtained with models in which the distribution in pitch angle α is proportional to $(\sin\alpha)^2 + 2(\sin\alpha)^{40}$ at the magnetic equator.[5, 9, 10, 7]

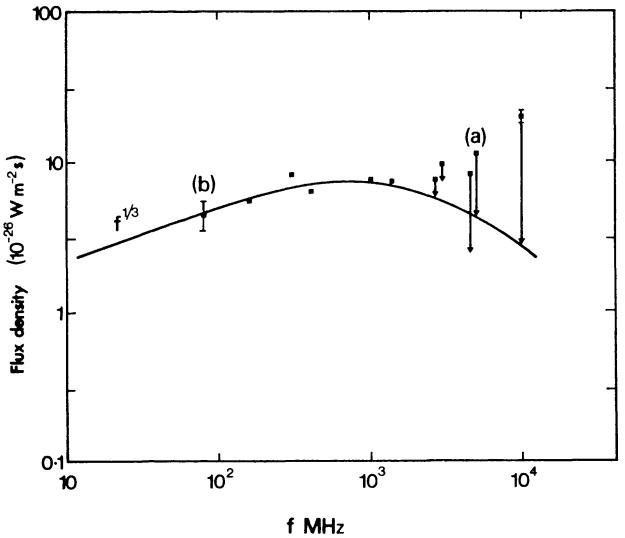

Figure 1. Showing the observations of flux density corrected (arrowed lines) for a disk temperature of 250°K to give the synchrotron component. The points at (a) 81.5 MHz, and (b) 5000 MHz, are the added ones referred to in the text.

Recently reported observations at 81.5 MHz[1] and at 5000 MHz[2, 3] have been added to those noted above and are shown in Figure 1. Following recent practice[2, 3, 11] we have corrected them for a disk temperature of 250°K instead of 140°K used by Roberts. A smooth spectrum curve has been drawn through the resulting points. This frequency spectrum is no longer flat but drops away at both low frequencies ($f < 500$ MHz) and high frequencies ($f > 1500$ MHz). On the basis of this spectrum we question the validity of assuming a flat synchrotron spectrum and hence also the validity of taking $\gamma = 1$ in the energy distribution function.

We have recently developed methods and computer programmes to calculate the emission from these dipolar models.[6, 11] New features are the inclusion of the effects of upper and lower limits (E_2, E_1) in the energy distribution and the inclusion of a first-harmonic cut-off. Quantitative examples suggest that the low frequency spectrum of Figure 1 can be accounted for by choosing E_1 appropriately, and that the high frequency part of the spectrum can be accounted for by a suitable combination of E_2 and γ.

Figure 2 exemplifies the complete frequency spectrum of the total flux from charged particles moving in dipolar magnetic fields,[11] including the effects of a lower limit in